A Novel Active Power Control System for Wind Turbines Capable of AGC and Primary Response

Jacob Aho* Lucy Pao† Andrew Buckspan*
University of Colorado Boulder, Boulder, CO, USA
Paul Fleming‡
National Renewable Energy Laboratory, Golden, CO, USA §

Wind energy is increasing penetration levels on utility grids as more wind turbines are being installed. As the penetration of wind energy increases, there is motivation for wind turbines to actively control their power output to meet power set points provided by grid operators and assist with frequency regulation. This paper focuses on the development of a novel wind turbine control system that is capable of varying the turbine's active power output upon receiving Automatic Generation Control (AGC), or power set-point, command signals to meet the system operators needs in below and above rated wind speeds. The turbine is de-rated to reach the set-points by achieving a higher than optimal tip speed ratio, storing additional inertia in the rotor which can be used to assist in frequency regulation by providing a primary/inertial response to fluctuations in grid frequency.

Nomenclature

β	blade pitch angle
C_p	Power coefficient
λ	tip speed ratio (TSR)
Ω_g	generator speed
τ_g	generator torque
AGC	automatic generation control
BPF	band-pass filter
$CART3$	3-bladed Controls Advanced Research Turbine
DEL	damage equivalent load
$ERCOT$	Electric Reliability Council of Texas
LPF	low-pass filter
$NREL$	National Renewable Energy Laboratory
P_{rated}	rated power of the turbine
TSO	transmission system (grid) operator

I. Introduction

Wind power installed capacity is experiencing a rapid growth rate, as in 2010 worldwide capacity grew by 23.6% [1]. Wind energy provided only 2.5% of the global electricity supply in 2010, but countries such as Denmark, Portugal, Spain, and Germany have high wind penetrations, producing 21%, 18%, 16%, and 9%

*Doctoral student, Dept. of Electrical, Computer, and Energy Engineering, CU Boulder, AIAA Student Member.
†Richard & Joy Dorf Professor, Dept. of Electrical, Computer, and Energy Engineering, CU Boulder, AIAA Member.
‡Research engineer, NREL National Wind Technology Center, AIAA Member.
§This paper is produced as part of the NREL Active Power Control from Wind Power Project. This work was supported in part by the U.S. Department of Energy's Office of Energy Efficiency and Renewable Energy Wind and Hydropower Technologies Program.

of their electrical energy from wind turbines, respectively [1]. The transmission system operators (TSOs) in areas with high wind penetrations have increased interest in wind turbines providing grid services such as meeting power set-points and providing automatic grid frequency regulation services, both done through active power control (APC).

Conventional electricity generators are typically required to provide active power control through several different regimes. These generators are capable of meeting the TSOs automatic generation control (AGC) commands, or power set-points, which are used to balance electrical supply and demand. The conventional generators are also usually required to automatically react to fluctuations in grid frequency to provide stability during transmission or generation faults. Any synchronous generator on the grid inherently provides inertial response by 'bogging down' and producing extra power extracted from the spinning inertia when there is a shortage of power supply. Many of these generators also have governors that increase or decrease power output temporarily when there is a decrease or increase in grid frequency. For more detail and further information of inertial, primary, and AGC response, see [2] and [3].

Historically, wind power has not provided grid regulation services, as most large scale modern turbines are de-coupled from the utility grid via their power electronics. Increasing wind penetrations on some grids has pushed the TSOs to set new requirements for wind turbines to provide active power control services. Such requirements include meeting AGC power set-points and reacting over a limited time frame to grid frequency events [4, 5, 6, 7, 8]. A schematic showing the interconnection of the TSO, utility grid, wind plant controller, and individual turbines can be seen in Fig. 1.

APC for wind turbines is now an active area of research in industry and academia. This paper focuses on the development of a readily deployable novel wind turbine control system that is capable of meeting AGC power reference commands and providing a primary/inertial response to grid frequency. Here we focus on the control system at an individual turbine level that directly receives AGC commands and measures the grid frequency.

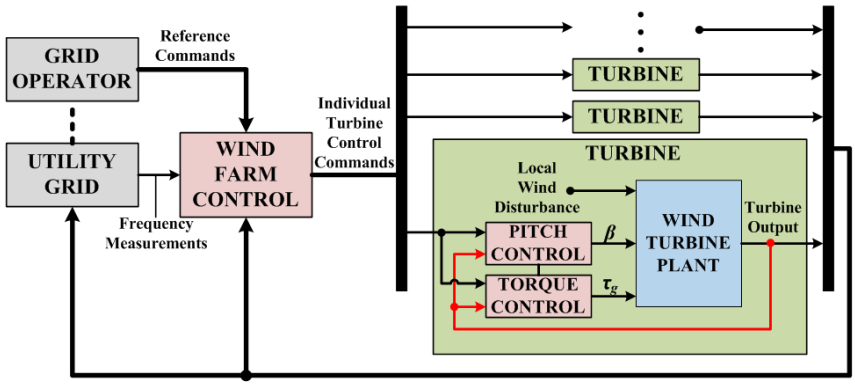

Figure 1. A schematic showing the interconnection between the TSO, or grid operator, AGC power reference commands, the grid frequency, the wind plant controller and the individual turbine. The wind plant controller receives the AGC commands and translates grid frequency into a change in power output and sends commands to the individual turbines. This paper focuses on the control system of an individual turbine. Figure used with permission from [9]

This paper is organized as follows. Section II describes the development of the control system. Section III presents selected simulation results highlighting the capability of the control system. Section IV provides concluding comments and discusses the ongoing work to be included in the final paper.

II. Control System Development

In this section, we briefly overview the goals of traditional wind turbine control systems and explain the development of a wind turbine controller that can meet AGC command signals and assist in frequency regulation by providing a primary/inertial response. First, the AGC baseline control system development is described by dividing the operation into below-rated-speed and rated-speed operation. We then explain the augmentation of this control system to be capable of reacting to frequency events via primary control.

The power available in a uniform wind field is $P_a = \frac{1}{2}\rho A v^3$, where P_a is the power $[W]$ of the wind with air density ρ $[kg/m^3]$ and wind speed v $[m/s]$ passing through the swept area A $[m^2]$ of a rotor disk that is perpendicular to the wind flow [10]. The wind turbine blades can only capture a fraction of the power available from the wind. The fraction of captured power to available power is referred to as the power coefficient $C_p(\beta, \lambda)$, which is a function of the tip-speed ratio (TSR) λ and the collective blade pitch β. The

TSR is the ratio of the tangential velocity of the blade tips divided by the wind speed perpendicular to the rotor plane. A characterization of a wind turbine's power coefficient C_p is shown as a contour plot in Fig. 2.

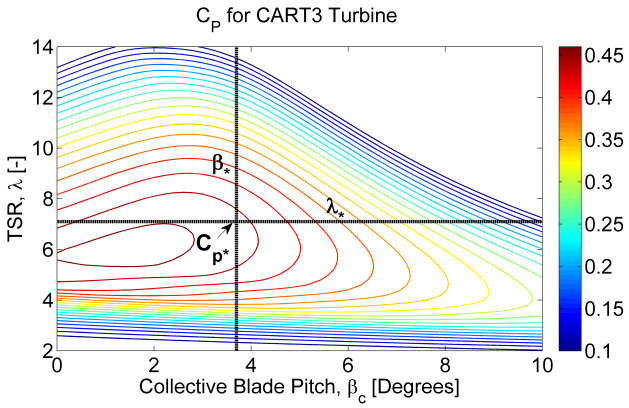

Figure 2. A characterization of the power coefficient C_p of the 3-bladed Controls Advanced Research Turbine (CART3) rotor. The dotted lines represent the tip-speed ratio λ_* and the collective blade pitch β_* that are maintained in below-rated conditions, resulting in the power coefficient C_{p*}. The operating point C_{p*} is not located at the maximum power capture point for this particular turbine so that the higher TSR will cause the turbine to reach rated speed before rated power, as is common with large-scale turbines.

The primary goal of traditional wind turbine control systems is to maximize power extraction in order to maximize profitability. This is done by maintaining the maximum power coefficient C_{p*} by keeping the blade pitch angle at β_* and controlling the generator torque to maintain the optimum tip speed ratio λ_*. To do this, the commanded generator torque τ_g is set to balance the steady-state aerodynamic torque according to

$$\begin{aligned} \tau_g &= K_* \Omega_g^2 \\ K_* &= \frac{1}{2}\rho A R^3 \frac{C_p(\beta_*, \lambda_*)}{{\lambda_*}^3 {N_{gear}}^3} \end{aligned}$$

where N_{gear} is the generator speed to rotor speed gear ratio (i.e., a constant greater than unity), Ω_g is the generator speed, ρ is density of the air, A is swept area of the rotor, R is the rotor radius, and (β_*, λ_*) are typically the blade pitch and TSR, respectively, where the power coefficient C_{p*} occurs [10]. It can be shown that this generator torque control law will balance the aerodynamic and load torques to regulate the speed of the turbine to the optimal TSR in steady-state conditions [11].

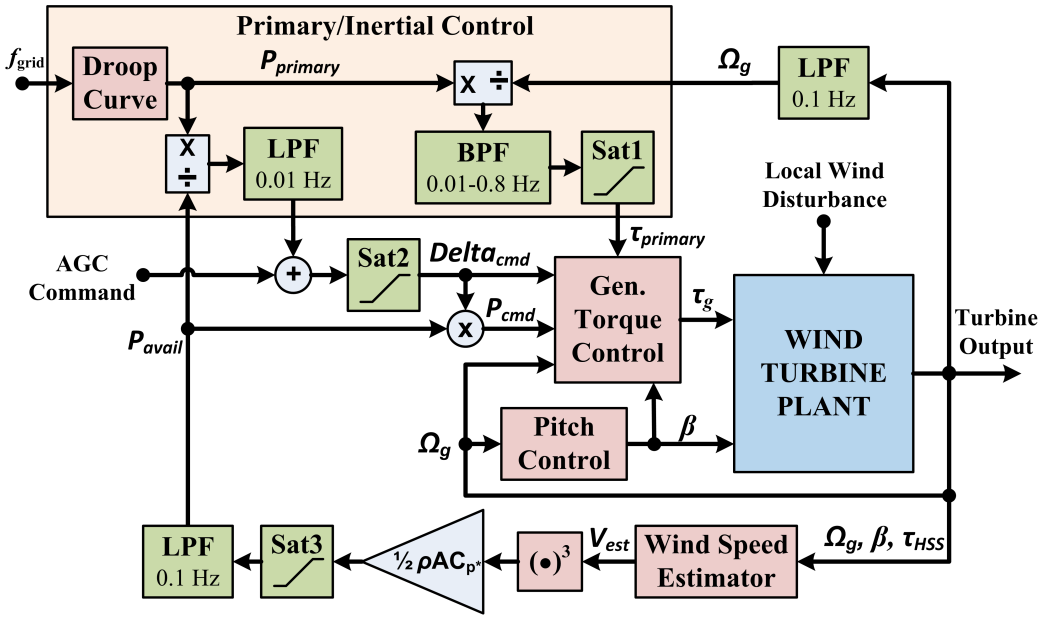

Figure 3. A block diagram of the control system including the baseline AGC power reference controller, primary/inertia controller, and wind speed estimator. The saturation blocks 'Sat1', 'Sat2' and 'Sat3' have saturation limits of $\pm 0.25\tau_{rated}$, $0-1$, and $0-P_{rated}$, respectively. All low-pass filters (LPF) are first-order and the band-pass filter (BPF) is second-order.

Once the wind turbine is operating at rated power, the primary goal of traditional control systems is to regulate the turbine power at the rated level. This is done by pitching the blades to shed extra aerodynamic power so that the turbine maintains rated speed. The generator torque is either held constant at the rated level, or controlled inversely proportional to generator speed to maintain rated power [12]. The blades are

pitched using a gain-scheduled proportional-integral (PI) control system that pitches the blades in reaction to generator speed error [12]. This type of blade pitch control system is used in this study and comprises the 'Pitch Control' block seen in Fig. 3.

A. Wind Speed Estimator

An estimator is developed to estimate the effective wind speed over the turbine rotor, and therefore the power available in the wind. A steady-state lookup table is used to provide these wind speed estimates, depicted in Fig. 3 as the 'Wind Speed Estimator' block. The wind speed lookup table is generated based on a power coefficient parametrization $C_p(\lambda, \beta)$, such as shown in Fig 2. For the C_p data and turbine model used in this study, there is a unique wind speed for a given rotor speed Ω_g, blade pitch β, and high-speed shaft torque τ_{HSS} while operating at steady state. By using sensors to measure these turbine states, the wind speed can be estimated by using a lookup table of $V_{est} = f(\Omega_g, \beta, \tau_{HSS})$. The simulated output of the wind speed estimator for above and below rated turbulent wind files is plotted against the hub height wind speed in Fig. 4.

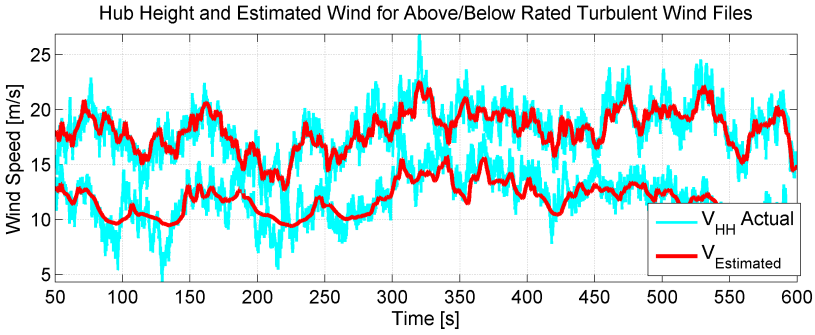

Figure 4. The performance of the wind speed estimator compared with the hub height wind speed during simulations with above and below rated turbulent wind files.

Since V_{est} is based on a lookup table of steady-state values, the estimate is more accurate when the turbine is operating at rated speed. This can be seen in Fig. 4 when the wind drops rapidly below 10 m/s and the turbine drops below rated speed. The errors induced during below-rated speed operation do not affect the controller performance in this study, since the wind speed estimate is only used to generate the torque command in rated-speed operation. The AGC command is set to 100% power for the simulations in which Fig. 4 was generated. The wind speed at which the turbine enters below-rated operation decreases when a lower AGC power reference is commanded. The power available in the wind is calculated based on the estimated wind speed and low pass filtered at 0.1 Hz to remove sensor noise and avoid high frequency actuation of the torque control system since the wind speed estimate is only used to capture a specified fraction of the power available from the wind.

B. Torque Control System Description

The torque control is divided into three separate sections, below-rated speed AGC torque control, rated speed AGC torque control, and the primary/inertial torque control. The primary goal of the AGC torque control systems is to track a power command signal from the transmission system operator. This signal may be an absolute power set-point or a delta command signal, which specifies a percentage of the power available in the wind to capture. This study focuses on reacting to a delta command signal, but the control system architecture is fully capable of receiving either type of command signal. A schematic of the control system developed for this study can be seen in Fig. 3. The control system is designed to be capable of receiving AGC power reference commands of any form, including step commands which are considered for this study. The torque control system is turned off when the rotor speed is spinning below 20% of rated speed.

1. Below-Rated Speed AGC Torque Control

The control system de-rates the power of the wind turbine in below-rated speed operation by varying the generator torque to obtain a sub-optimal TSR. In this region of operation the blades are kept at β_* due to the pitch control system that operates to prevent the turbine from exceeding rated speed. A method of de-rating the turbine in this manner was presented in [13] and [14], where the turbine operates at a higher than optimal tip-speed ratio. There are two rotor speeds that can achieve a particular de-rated power level for a given wind speed, as seen in Fig. 5 for wind speeds of 7 and 9 m/s. The controller tracks the higher of

these speeds so that there is more inertia stored in the rotor. This allows the primary/inertial component of the controller to react to an under frequency event by extracting some of the additional inertia and slowing the turbine down to operate at a higher power coefficient, as described in section 3 below. Though this method is presented in [13] and [14], these studies focus on the primary/inertial controls with a constant power AGC signal from a power electronics viewpoint and do not consider practical turbine speed limitations and interactions between the torque and pitch controllers.

It can be seen in Fig. 5 that for each constant derated power level, a different torque feedback gain K_{AGC} must be used to control the generator torque as $\tau_g = K_{AGC}\Omega_r^2$, as shown for the 'Max Power' and '80% Power' trajectories. A lookup table is generated to determine the appropriate feedback gain K_{AGC} for a given delta AGC power command signal. The feedback K_{AGC} gain is then low-pass filtered, as seen in Fig. 3, to avoid rapid torque actuation which will excite the turbine natural modes.

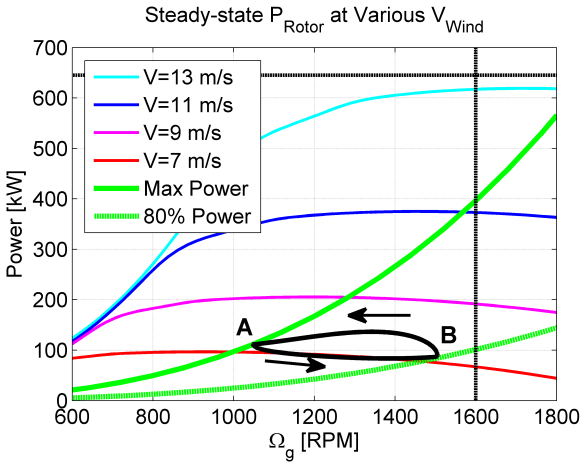

Figure 5. Various steady-state power capture curves for given wind speeds (V) at β_*. The 'Max Power' curve is the trajectory of the turbine that achieves C_{p*} for each wind speed by controlling the generator torque to be $\tau_g = K_*\Omega_g^2$. The '80% Power' curve is the trajectory that leaves 20% overhead power via rotor speed control and can be achieved by controlling generator torque as $\tau_g = K_{80\%}\Omega_g^2$. The black curve shows the turbine trajectories during transitions between 100% and 80% power at a constant wind speed of 7 m/s, which are labeled points A and B, respectively.

2. *Rated-Speed Operation AGC Torque Control*

Once the turbine reaches rated speed the blade pitch actuator becomes active to prevent rotor overspeed. To meet the AGC power set-point when operating at rated speed, the torque can be commanded to be the AGC absolute power command divided by the rated speed. The AGC absolute power command can be calculated from the AGC delta set-point if the power available from the wind is known. The wind speed, and hence available wind power, is estimated by using the technique described in section A above. The available power from the wind is saturated at the rated turbine power, and therefore the ratio of extracted power to rated power does not exceed the AGC delta command in steady-state operation. The AGC power command is low-pass filtered to avoid rapid torque actuation. The AGC power command can be tracked more rapidly than the power command when in below rated-speed operation where the feedback gain K_{AGC} must be changed slowly to avoid large power spikes, as will be shown in section III below.

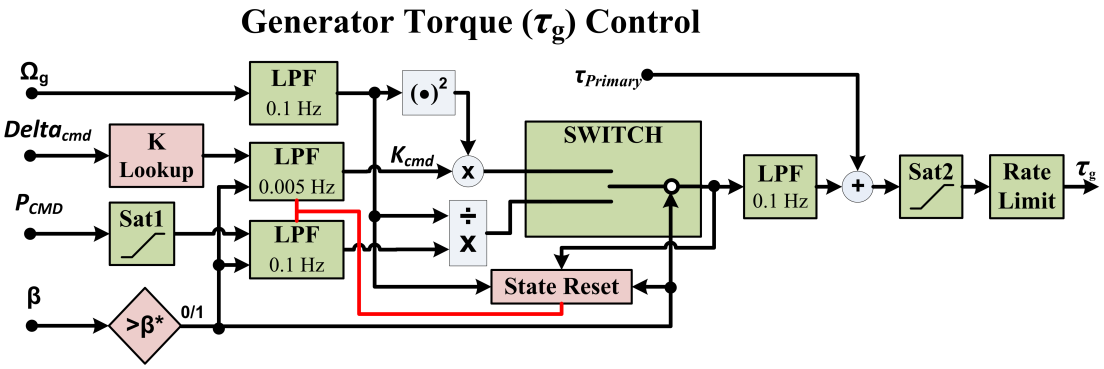

Figure 6. A detailed schematic of the generator torque τ_g controller block in Fig. 3. The switch is triggered when the blade pitch is at a value above β_* which also triggers the state reset of the low pass filters.

The AGC torque controller switches into rated-speed operation when the blades are pitched above β_*, as seen in Fig. 6. Because the output of the below-rated and rated torque controllers are not equal, a bumpless transfer technique is used to reset the states in the low-pass filters at either input of the switch shown in Fig. 6. The low-pass filters are implemented in state-space $\dot{x}_i = A_i x_i + B_i u_i, y_i = C_i x_i + D_i u_i$. Because the

low-pass filters are first-order, the C_i terms are scalar and the D_i terms are 0. Upon switching from channel i to j the state of channel j is reset to $x_j = \frac{f_j(y_i)}{C_j}$, where $f_j(\cdot)$ is either $\frac{y_i}{\Omega_g^2}$ or $y_i\Omega_g^2$ depending on whether the low-pass filter of K_{AGC} or P_{cmd} is being reset, respectively. The output of the switch is low pass filtered to further reduce high frequency torque actuation.

3. Primary/Inertial Response

There is motivation for wind turbines to provide frequency regulation services when a frequency event occurs on the grid. Over-frequency events may occur due to a loss of load and under-frequency events may occur due to a loss of generation. Since it is easier for a turbine to reduce power output due to an over-frequency event, we focus on under-frequency events, which requires the turbine to be de-rated so overhead power is available.

A droop curve is often used to parameterize the change in power output of a conventional generator governor due to a change in grid frequency. Here we use a static droop curve to synthesize a primary response in the wind turbine by converting measured grid frequency to a desired percentage of change in rated power of the turbine. For this study, a droop curve with a 5% slope is used to generate the primary power reference $P_{primary} = \frac{P_{rated}}{0.05}\frac{(60Hz - f_{grid})}{60Hz}$ and is saturated at $\pm 0.25P_{rated}$. A study has shown that using dynamically shaped droop curves that become more aggressive (steeper) with higher rates of change of frequency can effectively improve the primary/inertial response without significant increase of damaging loads on the turbine [15], but dynamic droop curves are not considered during this initial study.

The primary power reference $P_{primary}$, is split using a low-pass and band-pass filter, with the lower cutoff frequency of the band-pass filter equal to the cutoff frequency of the low-pass filter. The low-pass filtered component of $P_{primary}$ is normalized to the percentage of available power from the wind and added to the AGC delta power command. The band-pass filtered component of $P_{primary}$ is divided by the low-pass filtered rotor speed to acquire a perturbation torque command $\tau_{primary}$ that is added to the AGC torque control system command, as seen in Figs.3 and 6. The primary torque command is saturated at 25% of the rated torque and is turned off when the rotor speed is 20% of the rated speed.

III. Simulation Results

Simulations were performed with the FAST wind turbine response simulator developed at the National Renewable Energy Laboratory (NREL) National Wind Technology Center (NWTC) [16]. The FAST simulator uses blade element momentum theory to test aeroelastic models of a wind turbine with stochastic turbulent wind inflow files [16]. The turbine model used in this study is the NREL NWTC 3-bladed Controls Advanced Research Turbine (CART3) for which P_{rated} is 600 kW. The CART3 is a physical turbine on the NWTC site that is equipped with many sensors and has a computer capable of implementing custom control systems. All feedback signals used for the wind speed estimator and control system described in this paper are available on the CART3.

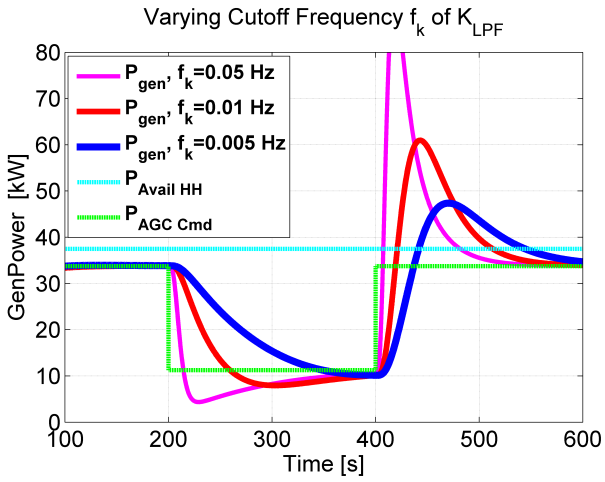

Figure 7. The effects of changing the K_{LPF} cutoff frequency during constant, below-rated winds (5 m/s) as the AGC power command signal is varied from 90% to 30% and back to 90%.

The design of many of the filters for this control system were intuitive with respect to the implications of the cutoff frequency and were designed conservatively to avoid rapid actuation of the generator torque. The design of the K_{LPF} low-pass filter provided particularly interesting tradeoffs. Simulation tests were performed under constant, uniform, below-rated wind of 7 m/s where the AGC command signal was stepped from 90% to 30% and back to 90%, as seen in Fig. 7. As the K_{LPF} cutoff frequency increases, the torque actuates more rapidly and provides a

large power dip and spike after the power command decrease and increase, respectively. A cutoff frequency of 0.005 Hz was chosen due to the rate of response and lack of excessive power overshoot.

Simulations were also performed under stochastic turbulent wind fields to analyze the damage equivalent loads (DELs) induced on the turbine components for varying levels of constant AGC delta set-points. The results of these simulations can be seen in Fig. 8. It can be seen that reducing the power set-point below 100% reduces the blade flap and tower side-side bending moments while slightly increasing the tower fore-aft bending moments. The fluctuations of the low-speed shaft flex were increased with lower AGC delta power commands, which should be addressed in future work.

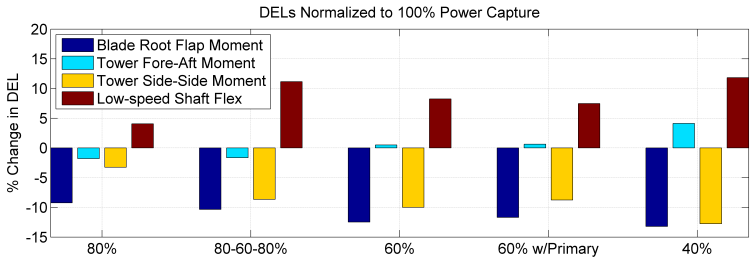

Figure 8. The induced damage equivalent loads on turbine components from above rated turbulent wind fields. The AGC delta command remained constant at the specified power level, except in the '80-60-80%' case, in which the AGC delta command was stepped from 80% to 60% and back to 80% for equal intervals of the simulations. The primary torque control system was only active in the '60% w/Primary' case.

Simulations were also performed to analyze the response of the primary component of the control system, as seen in Fig. 9. A frequency reference signal measured from a generator fault on the Electric Reliability Council of Texas (ERCOT) grid is passed through the turbine droop curve to generate the primary command signals. The turbine was simulated with an above-rated turbulent wind field and with a constant AGC command signal so that the variation of output power due to the primary response can be seen more clearly.

The control systems is also tested during a simulation performed with a turbulent wind field that is near the rated wind speed of the turbine, as seen in Fig. 10. The same ERCOT frequency reference of Fig. 9 is used to generate a primary power command. The AGC delta power command is stepped from 70% to 90% and back to 70% at time 200 s and 400 s, respectively as an example command in response to the frequency event.

IV. Conclusions and Ongoing Research

This paper presents a novel wind turbine control system that is capable of de-rating to meet AGC command set-points and provide primary response to assist in grid frequency regulation. There is an increasing demand for wind turbines to provide these services to support grid stability, particularly in areas of high wind penetration. The initial results from the developed control system are very promising. The controller successfully tracks the AGC power reference commands. The wind speed estimator works well when the turbine is operating at rated speed, which is when the wind speed estimates are used. The control system de-rates the turbine by over-speeding to a sub-optimal tip speed ratio when operating below rated rotor speed. This allows extra rotor inertia to be extracted in an under-frequency event while raising the steady-state power for primary control. When the turbine is operating at rated speed, the blade pitch controller successfully maintains rated speed while the torque is controlled to track the power reference. The transition between the below-rated speed and above-rated speed torque controllers is handled smoothly by using a bumpless transfer teqnique.

Additional on-going research results will be included in the final paper. Attempts will be made to reduce the drivetrain damage equivalent loads induced by de-rating the control system, as shown in Fig. 8. Adding a rate limiter to the output of the 'K Lookup' block of Fig. 3 will also be analyzed. It can be seen in Fig. 7 that a larger power spike occurs when increasing the AGC delta command using the same low-pass filter. It may be useful to implement rate limits on K_{AGC}, with a lower magnitude rate limit being applied on the positive side.

Research on providing active power control with wind turbines will be continued in the future. The presented control system achieves the design goals, but can still be improved. Future studies may explore using an adaptive controller to determine the appropriate values of K_{AGC}. Field tests of this control system will be conducted on the CART3 to show the functionality of the control system on a physical wind turbine.

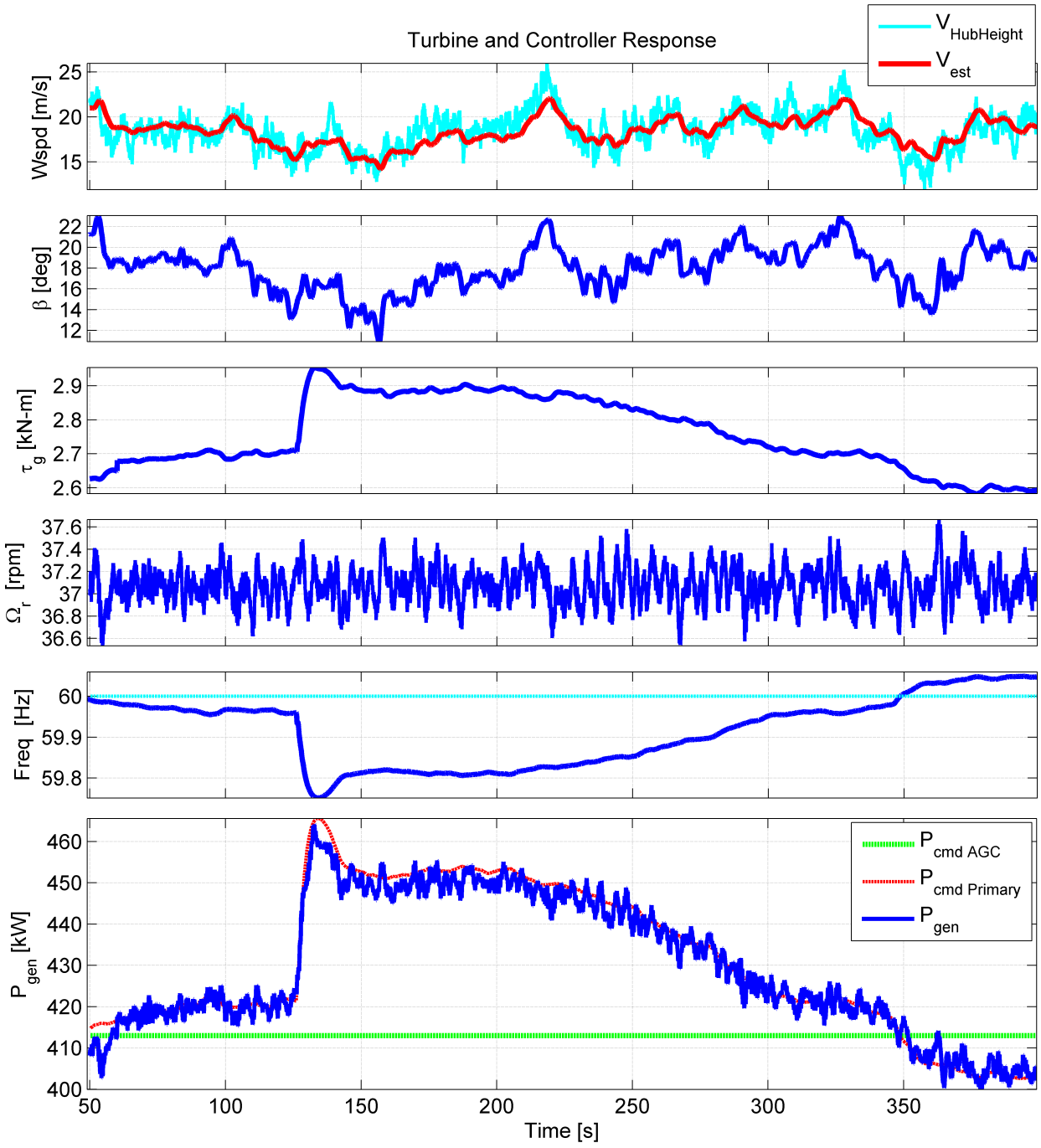

Figure 9. Simulation results for an above-rated wind field with a constant AGC delta command of 70% and a droop curve of 5% to show the primary/inertial response of the control system. A generation fault on the grid occurs at roughly 125 s where the grid frequency decreases rapidly. The decline in frequency is arrested by the inertia of the grid and is recovered slightly by the system primary response. The TSO AGC command increases the active power of generators on the grid, which is the reason for the frequency recovering to 60 Hz. Frequency event data is provided courtesy of Vahan Gevorgian (NREL).

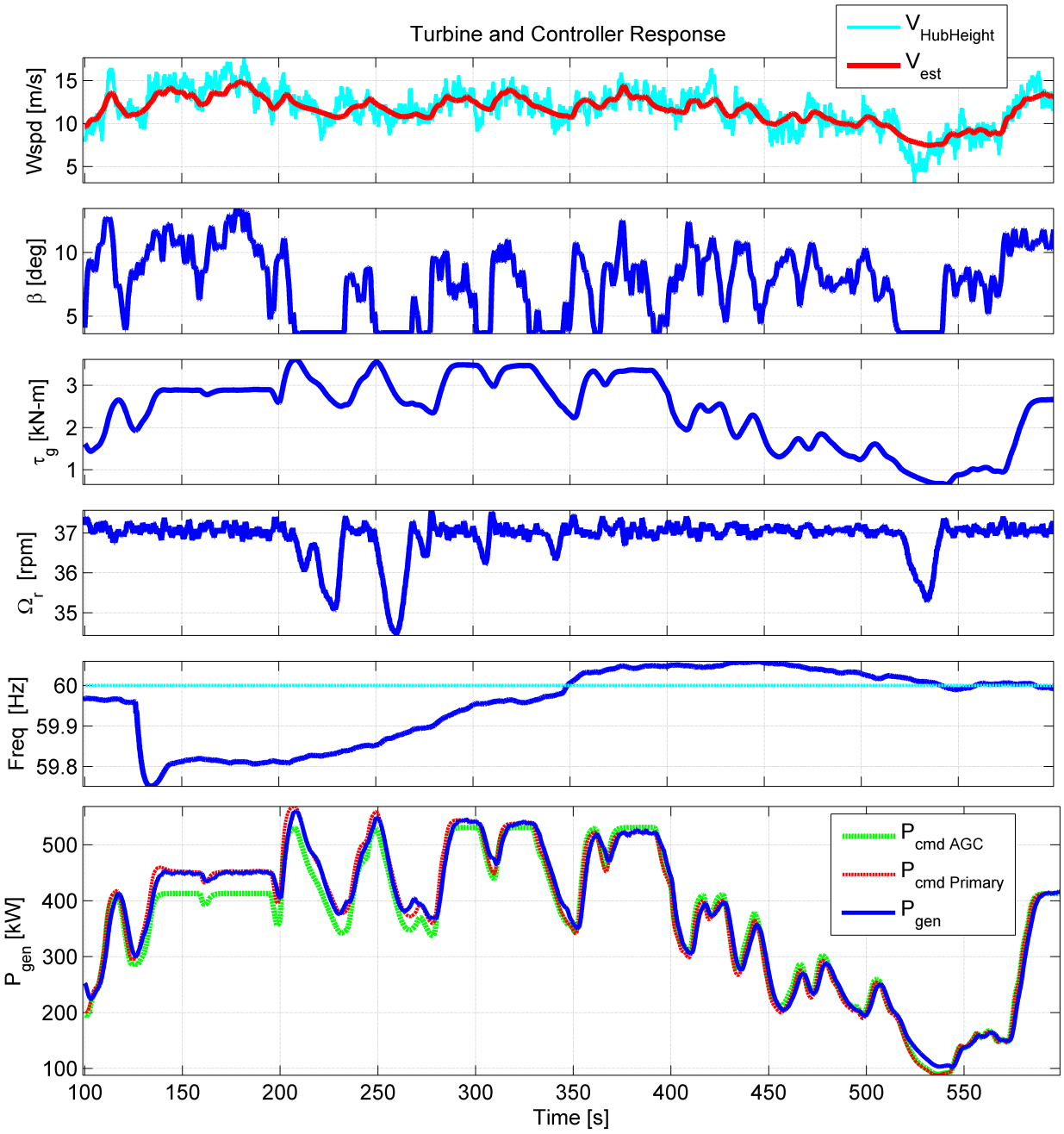

Figure 10. A simulation of the turbine and control system under turbulent winds showing AGC and primary capability. The AGC delta power commands are stepped from 70% to 90% and back to 70% at time 200 s and 400 s, respectively. The same frequency reference and 5% droop curve of Fig. 9 is used to generate the primary power command. The control system switches to below-rated operation when the blade pitch saturates at β_*, or 3.7 degrees.

References

[1] "World Wind Energy Report 2010," *Proc. 10th World Wind Energy Conference*, World Wind Energy Association, Cairo, Egypt, Nov. 2011.

[2] Rebours, Y., Kirschen, D., Trotignon, M., and Rossignol, S., "A Survey of Frequency and Voltage Control Ancillary Services-Part I: Technical Features," *IEEE Transactions on Power Systems*, Vol. 22, 2007, pp. 350–357.

[3] Ela, E., Milligan, M., and Kirby, B., "Operating Reserves and Variable Generation," Tech. rep., NREL/TP-5500-51928, 2011.

[4] Hansen, A. D., "Evaluation of power control with different electrical and control concepts of wind farms," Tech. rep., Project UpWind, Roskilde, Denmark, 2010.

[5] "Wind Farm Transmission Grid Code Provisions: A Direction by the Commission for Energy Regulation," Tech. rep., Commission for Energy Regulation, Dublin, Ireland, 2004.

[6] "Wind Turbines Connected to Grids with Voltages Above 100kV: Technical regulation for the properties and the regulation for wind turbines," Tech. rep., Elkraft System and Eltra, Erritsø, Denmark, 2003.

[7] "Technical Requirements for the Connection of Generation Facilites to the Hydro-Québec Transmission System: Supplementary Requirements for Wind Generation," Tech. rep., Hydro-Québec, Montreal, Québec, Canada, 2005.

[8] "Technical Requirements for Wind Power and Photovoltaic Installations and Any Generating Facilities Whose Technology Does Not Consist of a Synchronous Generator Directly Connected to the Grid," Tech. rep., Red Electrica, Madrid, Spain, 2008.

[9] Aho, J., Buckspan, A., Laks, J., Fleming, P., Dunne, F., Churchfield, M., Pao, L., and Johnson, K., "A Tutorial of Wind Turbine Control for Supporting Grid Frequency through Active Power Control," *Proc. American Control Conf.*, Jun. 2012.

[10] Manwell, J. F., McGowan, J. G., and Rogers, A. L., *Wind Energy Explained: Theory, Design and Application*, Wiley, 2009.

[11] Johnson, K., Pao, L., Balas, M., and Fingersh, L., "Control of variable-speed wind turbines: standard and adaptive techniques for maximizing energy capture," *IEEE Control Systems Magazine*, Vol. 26, No. 3, June 2006, pp. 70 – 81.

[12] Jonkman, J., Butterfield, S., Musial, W., and Scott, G., *Definition of a 5-MW Reference Wind Turbine for Offshore System Development*, National Renewable Energy Laboratory, Golden, CO, Feb. 2009.

[13] Ma, H. and Chowdhury, B., "Working Towards Frequency Regulation with Wind Plants: Combined Control Approaches," *Renewable Power Generation, IET*, Vol. 4, No. 4, July 2010, pp. 308–316.

[14] Juankorena, X., Esandi, I., Lopez, J., and Marroyo, L., "Method to Enable Variable Speed Wind Turbine Primary Regulation," *International Conference on Power Engineering, Energy and Electrical Drives*, March 2009, pp. 495–500.

[15] Buckspan, A., Aho, J., Fleming, P. Jeong, Y., and Pao, L., "Combining Droop Curve Concepts with Control Systems for Wind Turbine Active Power Control," *Proc. 2012 IEEE Symposium on Power Electronics and Machines in Wind Applications*, July 2012.

[16] Jonkman, J. and Buhl, M. L., *FAST User's Guide*, National Renewable Energy Laboratory, Golden, CO, 2005.